Title

Disordered amyloidogenic peptides may insert into the membrane and assemble into common cyclic structural motifs.

Journal

Chemical Society Reviews, 43(19)

Authors

Nussinov, Ruth
Jang, Hyunbum
Arce, Fernando
et al.

Publication Date

2014-10-07

DOI

10.1039/c3cs60459d

Peer reviewed

HHS Public Access

Author manuscript

Chem Soc Rev. Author manuscript; available in PMC 2015 October 07.

Published in final edited form as:

Chem Soc Rev. 2014 October 7; 43(19): 6750–6764. doi:10.1039/c3cs60459d.

Disordered amyloidogenic peptides may insert into the membrane and assemble into common cyclic structural motifs

Hyunbum Jang[a,*], **Fernando Teran Arce**[b], **Srinivasan Ramachandran**[b], **Bruce L. Kagan**[c], **Ratnesh Lal**[b], and **Ruth Nussinov**[a,d,*]

[a]Cancer and Inflammation Program, National Cancer Institute at Frederick, Leidos Biomedical Research, Inc., Frederick National Laboratory for Cancer Research, Frederick, Maryland 21702, U.S.A

[b]Departments of Bioengineering and of Mechanical and Aerospace Engineering, and Materials Science Program, University of California, San Diego, La Jolla, California 92093, U.S.A

[c]Department of Psychiatry, David Geffen School of Medicine, Semel Institute for Neuroscience and Human Behavior, University of California, Los Angeles, California 90024, U.S.A

[d]Department of Human Molecular Genetics and Biochemistry, Sackler School of Medicine, Tel Aviv University, Tel Aviv 69978, Israel

Abstract

Aggregation of disordered amyloidogenic peptides into oligomers is the causative agent of amyloid-related diseases. In solution, disordered protein states are characterized by heterogeneous ensembles. Among these, β-rich conformers self-assemble via a conformational selection mechanism to form energetically-favored cross-β structures, regardless of their precise sequences. These disordered peptides can also penetrate the membrane, and electrophysiological data indicate that they form ion-conducting channels. Based on these and additional data, including imaging and molecular dynamic simulations of a range of amyloid peptides, Alzheimer's amyloid-β (Aβ) peptide, its disease-related variants with point mutations and N-terminal truncated species, other amyloidogenic peptides, as well as a cytolytic peptide and a synthetic gel-forming peptide, we suggest that disordered amyloidogenic peptides can also present a common motif in the membrane. The motif consists of curved, moon-like β-rich oligomers associated into annular organizations. The motif is favored in the lipid bilayer since it permits hydrophobic side chains to face and interact with the membrane and the charged/polar residues to face the solvated channel pores. Such channels are toxic since their pores allow uncontrolled leakage of ions into/out of the cell, destabilizing cellular ionic homeostasis. Here we detail Aβ, whose aggregation is associated with Alzheimer's disease (AD) and for which there are the most abundant data. AD is a protein misfolding disease characterized by a build-up of Aβ peptide as senile plaques, neurodegeneration, and memory loss. Excessively produced Aβ peptides may directly induce cellular toxicity, even without the involvement of membrane receptors through Aβ peptide-plasma membrane interactions.

[*]Corresponding Authors: R.N., nussinor@helix.nih.gov; H.J., jangh2@mail.nih.gov.

Keywords

conformational disorder; intrinsically disordered peptides; ion-channel; cell membrane; molecular dynamics simulations; oligomers; bilayer; β-sheet; protein aggregation; amyloid; cell homeostasis

1. Introduction

Protein misfolding causes abnormal protein aggregates that link to fatal protein deposition diseases including a number of neurodegenerative diseases, such as Alzheimer's, Huntington's, Parkinson's, familial British dementia (FED), familial Danish dementia (FDD), and prion encephalopathies, type II diabetes and eye cataracts.[1–6] Amyloid aggregates are aging-related, symptomatically associated with Alzheimer's disease (AD), which is characterized by the presence of extracellular plaques, intracellular neurofibrillary tangles, and the loss of synapses and neurons in the brain of AD patients.[7,8] Despite the prevalence of amyloid-related diseases, their origins, mechanisms of toxicity, and how to prevent, halt or delay amyloidosis are still open questions. Common view has long held that protein misfolding-induced amyloids result in disease either by disrupting regular protein function or by inducing a gain-of-function, often causing pathophysiologic cell response by destabilizing cellular ionic homeostasis.[1–3] In solution, many of the amyloid aggregates form by disordered peptides (or fragments) assembling into a common, regular cross-β structures through conformational selection of preferred β conformers.[9]

The traditional amyloid hypothesis holds that accumulation of β-amyloid (Aβ) peptide in the brain is the primary cause of AD pathogenesis, leading to synapse loss and neuronal cell death.[10–14] The extracellular plaques mainly contain Aβ peptides and the intracellular tangles include aggregates of Tau protein.[4,5] Amyloid fibrils with a β-sheet pattern are commonly found in these aggregates, deposited both in the extracellular space and in the cytoplasm.[15,16] Early studies pointed to fibrillar deposits of Aβ peptides in the extracellular plaques as directly associated with the cause of the disease.[16] However, a long term clinical study revealed that even though an experimental drug (AN1792) could remove the extracellular plaques in AD patients, it failed to prevent progressive neurodegeneration.[17] The current amyloid cascade hypothesis in AD points to small Aβ oligomers as the main toxic species,[18–22] gradually shifting the research focus to Aβ oligomers rather than fibrils.[23,24] This hypothesis suggests that early stage symptoms of AD, including reduced synaptic function as well as impairment of learning and memory formation processes, are associated with oligomeric assemblies.[5,25] The interaction of Aβ with the cell membrane is a fundamental mechanistic chemical feature leading to AD pathogenesis.[26–29] Here, we suggest that small oligomers of Aβ and other disordered amyloidogenic peptides may insert into the membrane and assemble into common β-sheet rich annular structural motifs and review the literature in this light, focusing on Aβ which has abundant data.

The 39–43 (40 and 42 are the most common) amino acids long Aβ peptide is a fragment of the amyloid precursor protein (APP) (Fig. 1A). APP cleavage is driven by β-secretase (BACE) at position 1 outside the cell and γ-secretase at positions 40 or 42 within the cell membrane (Fig. 1B). While the production of $A\beta_{1\text{-}40}$ is energetically more favorable than $A\beta_{1\text{-}42}$, $A\beta_{1\text{-}42}$ is more toxic to neurons than $A\beta_{1\text{-}40}$.[30] In addition to the full-length $A\beta_{1\text{-}40/42}$

peptide, N-terminal truncated fragments are also formed via cleavage of the APP by β′- and γ-secretases producing the $A\beta_{11\text{-}40/42}$ peptide (Fig. 1C), and α - and γ-secretases cleavage yields $A\beta_{17\text{-}40/42}$ peptide (Fig. 1D).[11,31] Since these truncated peptides were putatively treated as nonpathogenic species, drugs to inhibit BACE were used to block production of the full-length Aβ peptides, and at the same time, enhance the production of the N-terminal truncated Aβ peptides.[32] However, recent studies using complementary techniques of atomic force microscopy (AFM), molecular dynamics (MD) simulations, planar lipid bilayer (PLB), cell calcium imaging, neuritic degeneration, and cell death assays demonstrated that the N-terminal truncated Aβ peptides, $A\beta_{17\text{-}42}$ (p3) and $A\beta_{9\text{-}42}$ (N9), formed toxic ion channels in the lipid bilayers.[33–38] In particular, the p3 peptide was reported to induce toxicity in AD and is known to be the main constituent of cerebellear preamyloid lesions in Down Syndrome (DS).[39–41]

In spite of over a century of research, there is still no strategy to prevent or cure the AD.[42,43] An important reason for this is the lack of knowledge of a high resolution structure based on x-ray diffraction for the toxic amyloid oligomers, hampering the development of therapeutic drugs.[44] Solution and solid state NMR (ssNMR), without and with coordinated metals such as zinc and copper, indicated a range of conformations,[45–52] as did other spectroscopic techniques,[53,54] and molecular dynamics simulations.[55–62] The different amyloid states emerging from these underscore the chemical nature of Aβ: a disordered peptide with energetically fairly similar conformational states separated by low barriers, with the prevailing states highly sensitive to conditions and the chemical environment: solution or bilayer, peptide concentration, presence of ions, membrane composition, cholesterol, metals, presence of other amyloids such as of Tau protein known to co-aggregate with Aβ, and other proteins, and more. Further, slight sequence alterations, such as those involving single point mutations and truncated peptides, taking place under physiological conditions and in disease, can also be expected to shift the free energy landscape of amyloids.[63,64] The different conformations may self-assemble into multiple oligomeric cross-β seed states, propagating into a broad range of fibrils, differing in their organizations and dimensions.[65–70] It can be expected that the range of currently observed conformations will increase. On a different resolution scale, a substantial body of evidence obtained by AFM techniques illustrated assembled channel-like oligomer structures for a series of different amyloids.[21,36,71–78] Electron microscopy (EM) also provided images of amyloid oligomers with doughnut-like structures.[79–81] Given these predicaments, the problem of predicting amyloid conformations using MD simulations, coarse grained, implicit, or explicit solvent description- in the solution state, without and with metal ions, on and in the membrane, in the presence and absence of AD-related mutations, and truncated fragments has drawn much attention.[82–102] Recently, a series of MD simulations provided insight into the molecular conformations of oligomeric Aβ channel structures at atomic-level resolution,[33–38,77,78,103–106] exhibiting that Aβ channels are heterogeneous, consisting of β-sheet-rich subunits with morphologies and dimensions in good agreement with the imaged AFM channels.[21,72,73]

We propose that heterogeneous, disordered amyloidogenic peptides with different sequences frequently insert into the membrane and assemble into channel structural motifs. Insertion may depend on the membrane composition and net charge, which varies across tissues and

organism types. We center on Aβ channel structures derived from modeling and MD simulations for Aβ sequences and monomer morphologies, and relate these to AD. Similar structural motifs were obtained by simulations for other amyloidogenic peptides (a fragment of β_2-microglobulin (K3)[75] and the human islet amyloid polypeptide (hIAPP)[84,107] and by AFM for a still broader range.[21] They were also obtained for the cytolytic antimicrobial peptide (AMP), protegrin-1 (PG-1),[108,109] and for a synthetic peptide which self-assembles into a hydrogel.[110] Unregulated toxic ion channels consisting of β-rich oligomers annularly associated and supported by their bilayer environment may be a preferred state for heterogeneous disordered peptides. In solution, aggregated amyloid states typically present the cross-β structures. In the membrane, small β-sheet rich subunits may insert and if their concentration is sufficiently high, oligomerize to form circular organization. In both, conformational and organizational details vary with the sequence and physical environment. The MD simulations described below were performed by the CHARMM[111] program with the NAMD code[112] on the Biowulf cluster (http://biowulf.nih.gov) at the NIH.

2. Mechanisms of Aβ toxicity

Pathological amyloid folding alters the three-dimensional conformations from soluble native structures[113,114] to insoluble non-native β-sheet-rich aggregates,[115,116] ranging from small oligomers to fibers.[117] Upon binding to the cell membrane, these conformational changes, catalyzed by the membrane, disrupt cellular function inducing cytotoxicity.[4,5,118] Aβ toxicity can be a direct consequence of ion channel formation.[119] Amyloid channels consist of small oligomers with a β-sheet motif, self-assembled around an aqueous cavity in the lipid environment. The formation of water cavity provides passage for unregulated ionic currents across the lipid membrane, destabilizing cellular ionic homeostasis. In the early 90's, Arispe *et al*.[120–124] first reported electrophysiology data of Aβ ion channels in the PLB (or BLM for black lipid membrane) neuron experiments, proposing the amyloid ion channel hypothesis. The measured ionic flux across the reconstituted membrane detected the emergence of stepwise ionic currents over time pointing to ion channels (Fig. 2A). The Aβ channels were cation-selective, voltage-independent and blocked by zinc[73,124–127] (Fig. 2B). Unlike typical regulated ion channels, Aβ channels exhibited multiple, large single channel conductances in the range of 0.4–4 nS, inducing an abrupt change in the cellular ionic concentration, leading to significant disruption of the membrane potential and loss of cellular homeostasis. Similar observations were made for other channel-forming amyloids including IAPP,[128–133] prion protein fragment,[134] polyglutamine,[135] β_2-microglobulin,[136] transthyretin (TTR),[137] and serum amyloid A (SAA).[138]

Indirect large oligomer-induced toxicity effects relate to neuronal oxidative stress, inflammation, or cell membrane-mediated signaling pathways.[139–141] An alternative hypothesis to explain disruption of cellular ionic homeostasis suggested that large amyloid oligomers cause mechanical damage to the cell membrane inducing membrane thinning with consequent nonselective ion leakage through the low dielectric barrier in the locally perturbed membrane.[142,143] Recently, amyloid fiber growth on the membrane surface was found to produce fragmentation of the cell membrane, inducing non-specific leakages.[144–147] All of these Aβ-induced effects, whether via channel formation, receptor-

mediated pathways, or membrane thinning destabilized the cellular ionic homeostasis, primarily by increased levels of intracellular calcium.

3. Structures of Aβ peptide

3.1 $A\beta_{1-42}$ vs. $A\beta_{1-40}$

Early nuclear magnetic resonance (NMR) data suggested that Aβ monomers were generally disordered in aqueous environments,[114,148] but recent studies indicate that they are partially-folded α-helical structures.[149–151] When aggregated into oligomers or fibrils, however, the helical intermediates convert into β-sheet-rich structures. Lührs *et al*.[152] reported the $A\beta_{1-42}$ fibril structure from a combination of hydrogen/deuterium-exchange NMR data, side-chain packing constraints from pairwise mutagenesis, ssNMR and EM (pdb id: 2BEG). They obtained the coordinates for residues 17–42, while the N-terminal coordinates (residues 1–16) were missing due to disorder (Fig. 3A). The monomer conformation in the fibril was U-shaped with a β-strand-turn-β-strand motif and a turn located at Ser26-Ile31 with an intermolecular salt bridge Asp23/Lys28. The U-shaped monomer topology of Aβ peptides has been first introduced for solvated oligomers of $A\beta_{16-35}$ through modeling and MD simulations.[153] The peptides with the β-strand-turn-β-strand motif assembled in register presenting a parallel organization with the intramolecular salt bridge of Asp23/Lys28. Similar U-shaped peptides could be observed in small $A\beta_{1-40}$ protofibrils (pdb ids: 2LMN and 2LMO) defined by solid state NMR (ssNMR).[67] The U-shaped $A\beta_{1-40}$ peptide had a turn at Asp23-Gly29 and the same salt bridge as the $A\beta_{16-35}$ peptide (Fig. 3B). The N-terminal coordinates (residues 1–8) were missing due to disorder. Recently, another U-shaped $A\beta_{1-40}$ peptide[154] with a turn at Val24-Ala30, which is similar to the previous $A\beta_{1-40}$ model,[67] was reported. Combined, it appears that the more C-terminal turn at Asp23-Gly29 is an intrinsic turn of $A\beta_{1-40}$. In contrast, $A\beta_{1-42}$ preferentially adopted the less C-terminal turn at Ser26-Ile31.[152] Variants with additional turns near the C-terminal have also been detected, primary among these are those seeded from the brain extracts of two Alzheimer's disease patients presenting a triangular shape organization[155] reminiscent of earlier triangular organizations.[65,70]

3.2 Two $A\beta_{1-42}$ conformers derived from the NMR-based structures

The NMR-derived models of small $A\beta_{1-40/42}$ protofibrils only provided the N-terminal truncated Aβ coordinates due to conformational disorder.[67,152,154] In order to paint a complete picture for Aβ toxicity involving full-length Aβ peptides, structural information of the β-sheet peptide is needed.[156–159] Recently, computational modeling provided two U-shaped monomer conformations of $A\beta_{1-42}$ based on the NMR structures.[77,78,103,104] In the MD simulations, the $A\beta_{1-16}$ coordinates in the absence of Zn^{2+} (pdb id: 1ZE7)[47] were used for the missing N-terminal portions of the peptides.[67,152] For each combination of the N-terminal structure with the U-shaped motifs of $A\beta_{17-42}$ and $A\beta_{9-40}$, two $A\beta_{1-42}$ conformers were generated (Fig. 4). Conformer 1 has a turn at Ser26-Ile31, and conformer 2 at Asp23-Gly29. In the latter conformer, two C-terminal residues, Ile41 and Ala42 were added to create $A\beta_{1-42}$. Both $A\beta_{1-42}$ conformers retained the U-shaped β-strand-turn-β-strand motif and can be divided into four domains: the N-terminal fragment (residues 1–16 and 1–8 for conformer 1 and 2, respectively), pore-lining β-strand (residues 17–25 and 9–22 for

conformer 1 and 2, respectively), turn (residues 26–31 and 23–29 for conformer 1 and 2, respectively), and C-terminal β-strand (residues 32–42 and 30–42 for conformer 1 and 2, respectively).

4. Aβ channels in the lipid bilayers

4.1 N-terminal truncated $Aβ_{17-42}$ and $Aβ_{9-42}$ channels

APP cleavages by combinations of β′-/γ-secretases and α-/γ-secretases produce $Aβ_{11-42}$ and $Aβ_{17-42}$ (p3) peptides, respectively (Fig. 1C,D).[11,31] Adding two more residues to the N-terminal of $Aβ_{11-42}$ peptide obtains the $Aβ_{9-42}$ (N9) peptide. The pioneering computational studies of amyloid ion channels in the lipid bilayer have begun with these N-terminal truncated Aβ peptides.[33–38] The NMR-based U-shaped Aβ peptides[67,152] were directly employed in the modeling of the channels. Annular β-sheets in the channel and barrel topologies were initially constructed in a lipid environment as starting points for the explicit MD simulations. To construct the initial channel structure with conventional β-strands arrangement, 12-36 U-shaped peptides were inserted without inclination with respect to the membrane normal, generating the channel topology (Fig. 5A).[33–37] To construct the barrel structure, the U-shaped peptides were inclined ~37° relative to the pore axis and then a 12–20 fold rotational symmetry operation was performed with respect to the pore axis, creating the barrel topology (Fig. 5B).[38] In both topologies, the polar/charged N-terminal β-strands (residues 17–25 for p3 and 9–22 for N9 topologies) encompassed the water pore, and the hydrophobic C-terminal β-strands (residues 32–42 for p3 and 30–42 for N9 topologies) faced lipids. Other β-sheet-forming peptides also exhibited the channel and barrel topologies (Fig. 5C–E).

The annular channels/barrels gradually relaxed toward heterogeneous shapes in the lipid bilayer during the simulations (Fig. 6). The simulations illustrated that the Aβ channels and barrels consist of loosely attached β-sheet-rich subunits with the morphologies and dimensions in good agreement with the imaged AFM channels.[36] The outer dimensions and the pore diameters for the p3 and N9 channels/barrels from the simulations depended on the number of peptides assembled in the channels/barrels (Tables 1 and 2); however, the number of subunits which were formed during the simulations reflected the fluidic bilayer dynamics. Remarkably, the MD simulations presented optimal toxic ion channel sizes ranging between 16 and 24 monomers.[35,37] This range was also found to hold for other toxic β-sheet channels; 24-mer K3 (a fragment of $β_2$-microglobulin) channels with 24 β-strands,[75] 8-/10-mer protegrin-1 (PG-1) channels with 16–20 β-strands,[108,109] 18-/24-mer human islet amyloid polypeptide (hIAPP) channels with 18–24 β-strands,[107] and 10-mer for the synthetic hydrogel-forming peptide MAX barrels with 20 β-strands.[110]

4.2 L- and D-enantiomers $Aβ_{1-42}$ channels

The indirect mechanism for Aβ-mediated destabilization of ionic homeostasis suggested that Aβ binds to cell membrane receptors via stereospecific interactions, resulting in opening existing ion channels or transporters.[115,139] Cell binding studies by Ciccotosto *et al.*[160] showed that although both all L- and all D-amino acids $Aβ_{1-42}$ peptides (L-$Aβ_{1-42}$ and D-$Aβ_{1-42}$ peptides) bound to cultured cortical neurons, only the L-$Aβ_{1-42}$ peptide was

neurotoxic, suggesting stereospecific interactions of L-Aβ_{1-42} peptide. However, stereospecificity could be studied through comparison of the biological activities of the L- and D-enantiomers, since putative cellular receptors would not bind the D-Aβ due to the lack of conformational fitting. Recent comprehensive studies including AFM, PLB, and MD simulations demonstrated that the D-Aβ isomer formed ion channel in the bilayer with size, shape, and ion conductance behavior indistinguishable from the wild type L-Aβ isomer.[77,103] This suggested that Aβ toxicity occurred via a receptor independent, nonstereoselective mechanism. In the computational studies, the L- and D-enantiomers ion channels were modelled using two Aβ_{1-42} conformers (Fig. 4) with the β-strand-turn-β-strand motif. The D-Aβ_{1-42} conformers were mirror images of L-Aβ_{1-42}, obtained by reflecting the L-coordinates with respect to the reference plane (Fig. 7). The conformers retained the U-shaped β-strand-turn-β-strand motif similar to their L-Aβ_{1-42} counterparts, regardless of their chirality. Conformer 1 D-Aβ_{1-42} had a turn at Ser26-Ile31 and conformer 2 D-Aβ_{1-42} at Asp23-Gly29, following the wild type ssNMR models. 18-mers, L- and D-enantiomers Aβ_{1-42} barrels were simulated in an anionic lipid bilayer containing 1,2-dioleoyl-sn-glycero-3-phosphoserine (DOPS) and 1-palmitoyl-2-oleoyl-sn-glycero-3-phosphoethanolamine (POPE) with a mole ratio DOPS:POPE=1:2, and a zwitterionic lipid bilayer composed of 1,2-dioleoyl-sn-glycero-3-phosphocholine (DOPC).

During the simulations, the Aβ barrels were gradually relaxed through their interaction with the surrounding lipids, presenting the assembled-subunits channel morphology (Fig. 8A–D). Regardless of the D- and L-amino acids chirality, both Aβ conformers and isomers preserved the barrel conformation in a way such that the membrane-embedded, pore-lining β-strands encompassed the solvated pore, and the C-terminal β-stands interacted with lipid tails. The N-terminal portions were disordered and stayed extramembranous. The computational studies verified that D-Aβ_{1-42} was able to form ion channels and be active independent of stereospecific receptor interactions, presenting indistinguishable pore structures formed by both isomers as imaged by AFM (Fig. 8E). No differences in the calculated outer and pore dimensions for the Aβ_{1-42} barrels between different Aβ conformers and/or between different Aβ isomers were observed (Table 3).

4.3 Aβ mutants: F19P, F20C, and Osaka mutant (ΔE22) channels

Several point mutations linked to AD occur naturally in the Aβ peptide, clustered around the central region of the peptide.[11,161] These include the Flemish (A21G),[162] Artic (E22G),[163] Italian (E22K),[164] Dutch (E22Q),[162,164,165] and Iowa (D23N)[166] mutants. Since they affect the salt bridge in the turn region, several studies, experimental and computational, probed these substitutions in a water environment to understand their conformational consequences.[55,167–174] In addition, a designed synthetic proline substitution in the central region for a Phe residue is of particular interest, since proline is a β-sheet breaker, preventing the Aβ propagation into β-sheet-rich oligomers or fibrils.[175,176] The distinct behavior of the proline substitution in the Aβ channels indicated that substitution of Phe19 with Pro (F19P) in both truncated p3 (Aβ_{17-42}) and full-length Aβ_{1-42} channel/barrel conformations prevented pore activity and hence cellular toxicity.[36,78,104] Computational studies of these F19P mutant channels/barrels verified that kinks at Pro19 destabilized an inner β-sheet formed by the pore-lining β-strands (Fig. 9A). As a result, the F19P

substitution induced collapsed pores which prevented ions permeating across the bilayer. However, unlike the collapsed pore induced by the F19P substitution, the F20C substitution preserved the solvated pore with channel activity comparable to the wild type (Fig. 9B). Both F19P and F20C, channels and barrels, presented outer diameters in the wild type range, while the pore sizes significantly decreased for the F19P and slightly reduced for the F20C (Table 4).

Another mutation in the central region of the Aβ peptide, nicknamed the Osaka mutation, is a deletion of Glu22 (ΔE22).[177] It was known that Aβ mutants with a familial Alzheimer's disease (FAD)-linked point substitutions at Glu22 were toxic species.[178] Like these point substitutions, the complete elimination of the Glu22 position, rather than an amino acid substitution, is still linked to FAD. Recent computational studies provided a membrane-bound conformation of the ΔE22 barrel in atomic-level detail,[106] demonstrating that the mutant barrels presented similar morphologies and dimensions as those of the wild type $Aβ_{1-42}$ (Fig. 10 and Table 4). This suggested that the Osaka mutant could directly relate to the Aβ ion channel-mediated mechanism as observed for the wild type Aβ peptide in AD pathology.

4.4 $Aβ_{pE3-42}$ channels

Pyroglutamate (pE) modified Aβ peptides, in particular, the $Aβ_{pE3-42}$ peptide have been increasingly associated with enhanced toxicity, possibly due to its increased stability and higher aggregation propensity.[179,180] This peptide is generated post-translationally by cleavage of the first two N-terminal amino acids of $Aβ_{1-42}$, leaving an exposed glutamate (E) residue in position 3. The pyroglutamate (pE) ring is subsequently generated by intramolecular dehydration catalyzed by the glutaminyl cyclase (QC) enzyme.[179] Our preliminary AFM results indicate that the $Aβ_{pE3-42}$ peptide is able to form a channel in the lipid bilayer, with similar characteristics and dimensions as the channels observed in previous studies.[77,78] Subsequent MD studies also provide a model of $Aβ_{pE3-42}$ barrel in atomic details (Fig. 11).

5. Conclusions

Although the molecular mechanisms of Aβ that lead to cellular dysfunction are still unclear, they involve interactions of oligomeric species with the cell membrane.[19] Lipids and amyloid peptides can reciprocally affect their respective conformations. Aβ peptides have the potential to affect the structural integrity of the membrane, ultimately leading to cytotoxicity. Conversely, lipid membranes can promote the conversion of amyloid monomers into β-sheet-rich toxic oligomeric species.[29,181] Aβ membrane binding and insertion suggested that β-sheet oligomers spontaneously inserted to form membrane-bound aggregates.[159] These aggregates in the membrane were cytotoxic, and their presence, validated by electrophysiological recordings, set the amyloid channel hypothesis.[120,121] Amyloid channels were stable over time with lifetimes ranging from several minutes to hours. The cationic selective channels were voltage independent and blocked by zinc, presenting multiple interconverting conductance levels, suggesting that Aβ-mediated permeabilization is specifically caused by formation of intrinsic calcium permeable membrane pores.[182]

Several AFM structural studies have shown doughnut-like amyloid channels in lipid bilayers with outer diameters typically raging between 8–12 nm and inner diameters of ~2 nm.[21,72–74] Unlike typical ion channels, which have a well-defined number of subunits, amyloid channels present a varying number of subunits, ranging between trimers and hexamers.[77] Subsequent MD simulations provided amyloid channel conformations in atomic-level detail.[33–38,75,77,78,103,104,106] These computational channels were modeled using the U-shaped Aβ peptide with the β-strand-turn-β-strand motif. In the simulated channels, the solvated pore was lined by the central β-strands containing polar/charged residues, while the hydrophobic C-terminal strands interacted predominantly with the lipids. The modeled channels exhibited the water pore, wide enough for multiple ions to simultaneously enter and exit.

Given their prevalence, disordered states have been of increasing interest. Amyloidogenic deposits typically arise from disordered peptide species or fragments of amyloidogenic proteins. Disordered states are characterized by broad ensembles with no clear, highly populated state. Within the ensembles there are also β-rich conformers, and these associate through hydrophobic interactions and favorable generic backbone hydrogen bonds. The regular self-assembled structures permit seed formation which can propagate to form long and branched aggregates. The common occurrence of these in solution as a typical organization, irrespective of precise sequence reflects the cross-β stability. Peptides have long been known to insert into membranes. Here we posited that in membrane environments disordered peptides similarly tend to form common favored motifs. While here we focused on Aβ, we detailed their occurrence for Aβ variants – mutational and truncated species, as well as other amyloidogenic peptides, a cytolytic peptide and a synthetic gel-forming peptide. The fact that if the concentration of the disordered peptides is sufficiently high they tend to form annular organizations in membrane environments is not surprising: channels allow outer facing hydrophobic residues to favorably interact with the lipid membrane environment, and charged/polar residues to face a solvated water pore. Certain polar lipid-facing side chains in the β-strand can still be satisfied by some water molecules that permeate the membrane. This dislike of a membrane environment by the charged/polar surfaces already induces curvature to the oligomers, shrinking these exposed surfaces and expanding the membrane-loving hydrophobic, outer-surfaces, preorganizing the oligomers for channel formation. On the down side, while energetically favorable, such channels are toxic, since they permit unregulated passage of ions in their solvated pores, thus disturbing the cellular ionic homeostatis.

Although there has been significant support for the Aβ channel conformation consisting of the U-shape motif, this does not necessarily imply that such conformational species are always the preferred conformational states. The amyloid landscape is highly heterogeneous and different channel conformations may be populated.[9,44,63] Highly polymorphic membrane-permeated channels could evolve from different seed formations.[105,159] Whether these channels assembled in identical shape in the membrane or not, abundant structural evidence for Aβ channels with the β-sheet morphology by AFM and MD studies strongly suggests that a direct mechanism for the loss of cell ionic homeostasis in AD may also be operable in the cell.[126,183]

Acknowledgments

This project has been funded in whole or in part with Federal funds from the Frederick National Laboratory for Cancer Research, National Institutes of Health, under contract HHSN261200800001E. This research was supported [in part] by the Intramural Research Program of NIH, Frederick National Lab, Center for Cancer Research. The content of this publication does not necessarily reflect the views or policies of the Department of Health and Human Services, nor does mention of trade names, commercial products or organizations imply endorsement by the US Government. All simulations had been performed using the high-performance computational facilities of the Biowulf PC/Linux cluster at the National Institutes of Health, Bethesda, MD (http://biowulf.nih.gov).

References

1. Cohen FE, Kelly JW. Nature. 2003; 426:905–909. [PubMed: 14685252]
2. Temussi PA, Masino L, Pastore A. Embo J. 2003; 22:355–361. [PubMed: 12554637]
3. Dobson CM. Nature. 2003; 426:884–890. [PubMed: 14685248]
4. Chiti F, Dobson CM. Annu Rev Biochem. 2006; 75:333–366. [PubMed: 16756495]
5. DeToma AS, Salamekh S, Ramamoorthy A, Lim MH. Chem Soc Rev. 2012; 41:608–621. [PubMed: 21818468]
6. Eisenberg D, Jucker M. Cell. 2012; 148:1188–1203. [PubMed: 22424229]
7. Monsonego A, Zota V, Karni A, Krieger JI, Bar-Or A, Bitan G, Budson AE, Sperling R, Selkoe DJ, Weiner HL. J Clin Invest. 2003; 112:415–422. [PubMed: 12897209]
8. Di Paolo G, Kim TW. Nature Rev Neurosci. 2011; 12:284–296. [PubMed: 21448224]
9. Ma B, Nussinov R. Journal of molecular biology. 2012; 421:172–184. [PubMed: 22119878]
10. Tanzi RE, Bertram L. Cell. 2005; 120:545–555. [PubMed: 15734686]
11. Iversen LL, Mortishiresmith RJ, Pollack SJ, Shearman MS. Biochem J. 1995; 311:1–16. [PubMed: 7575439]
12. Jakob-Roetne R, Jacobsen H. Angewandte Chemie International Edition. 2009; 48:3030–3059.
13. Hardy. Current Alzheimer Research. 2006; 3:71–73. [PubMed: 16472206]
14. Hardy JA, Higgins GA. Science. 1992; 256:184–185. [PubMed: 1566067]
15. Sunde M, Blake C. Adv Protein Chem. 1997; 50:123–159. [PubMed: 9338080]
16. Sipe JD, Cohen AS. J Struct Biol. 2000; 130:88–98. [PubMed: 10940217]
17. Holmes C, Boche D, Wilkinson D, Yadegarfar G, Hopkins V, Bayer A, Jones RW, Bullock R, Love S, Neal JW, Zotova E, Nicoll JAR. Lancet. 2008; 372:216–223. [PubMed: 18640458]
18. Bernstein SL, Dupuis NF, Lazo ND, Wyttenbach T, Condron MM, Bitan G, Teplow DB, Shea JE, Ruotolo BT, Robinson CV, Bowers MT. Nature Chem. 2009; 1:326–331. [PubMed: 20703363]
19. Butterfield SM, Lashuel HA. Angewandte Chemie International Edition. 2010; 49:5628–5654.
20. Glabe CG. J Biol Chem. 2008; 283:29639–29643. [PubMed: 18723507]
21. Quist A, Doudevski I, Lin H, Azimova R, Ng D, Frangione B, Kagan B, Ghiso J, Lal R. Proc Natl Acad Sci USA. 2005; 102:10427–10432. [PubMed: 16020533]
22. Matsumura S, Shinoda K, Yamada M, Yokojima S, Inoue M, Ohnishi T, Shimada T, Kikuchi K, Masui D, Hashimoto S, Sato M, Ito A, Akioka M, Takagi S, Nakamura Y, Nemoto K, Hasegawa Y, Takamoto H, Inoue H, Nakamura S, Nabeshima Y, Teplow DB, Kinjo M, Hoshia M. J Biol Chem. 2011; 286:11555–11562. [PubMed: 21292768]
23. Klein WL, Krafft GA, Finch CE. Trends Neurosci. 2001; 24:219–224. [PubMed: 11250006]
24. Lambert MP, Viola KL, Chromy BA, Chang L, Morgan TE, Yu JX, Venton DL, Krafft GA, Finch CE, Klein WL. J Neurochem. 2001; 79:595–605. [PubMed: 11701763]
25. Haass C, Selkoe DJ. Nature Revs Mol Cell Biol. 2007; 8:101–112. [PubMed: 17245412]
26. Chi EY, Ege C, Winans A, Majewski J, Wu GH, Kjaer K, Lee KYC. Proteins. 2008; 72:1–24. [PubMed: 18186465]
27. Relini A, Cavalleri O, Rolandi R, Gliozzi A. Chem Phys Lipids. 2009; 158:1–9. [PubMed: 19056366]
28. Garner B. Biochim Biophys Acta. 2010; 1801:747–749. [PubMed: 20547302]
29. Williams TL, Serpell LC. FEBS J. 2011; 278:3905–3917. [PubMed: 21722314]

30. Singh R, Barman A, Prabhakar R. J Phys Chem B. 2009; 113:2990–2999. [PubMed: 19708161]
31. Thinakaran G, Koo EH. J Biol Chem. 2008; 283:29615–29619. [PubMed: 18650430]
32. Postina R, Schroeder A, Dewachter I, Bohl J, Schmitt U, Kojro E, Prinzen C, Endres K, Hiemke C, Blessing M, Flamez P, Dequenne A, Godaux E, van Leuven F, Fahrenholz F. J Clin Invest. 2004; 113:1456–1464. [PubMed: 15146243]
33. Jang H, Zheng J, Nussinov R. Biophys J. 2007; 93:1938–1949. [PubMed: 17526580]
34. Jang H, Zheng J, Lal R, Nussinov R. Trends Biochem Sci. 2008; 33:91–100. [PubMed: 18182298]
35. Jang H, Arce FT, Capone R, Ramachandran S, Lal R, Nussinov R. Biophys J. 2009; 97:3029–3037. [PubMed: 19948133]
36. Jang H, Arce FT, Ramachandran S, Capone R, Azimova R, Kagan BL, Nussinov R, Lal R. Proc Natl Acad Sci USA. 2010; 107:6538–6543. [PubMed: 20308552]
37. Jang H, Arce FT, Ramachandran S, Capone R, Lal R, Nussinov R. J Phys Chem B. 2010; 114:9445–9451. [PubMed: 20608696]
38. Jang H, Arce FT, Ramachandran S, Capone R, Lal R, Nussinov R. J Mol Biol. 2010; 404:917–934. [PubMed: 20970427]
39. Gowing E, Roher AE, Woods AS, Cotter RJ, Chaney M, Little SP, Ball MJ. J Biol Chem. 1994; 269:10987–10990. [PubMed: 8157623]
40. Higgins LS, Murphy GM, Forno LS, Catalano R, Cordell B. Am J Pathol. 1996; 149:585–596. [PubMed: 8701997]
41. Lalowski M, Golabek A, Lemere CA, Selkoe DJ, Wisniewski HM, Beavis RC, Frangione B, Wisniewski T. J Biol Chem. 1996; 271:33623–33631. [PubMed: 8969231]
42. Lansbury PT, Lashuel HA. Nature. 2006; 443:774–779. [PubMed: 17051203]
43. Hardy J. Neuron. 2006; 52:3–13. [PubMed: 17015223]
44. Jang H, Connelly L, Arce FT, Ramachandran S, Lal R, Kagan BL, Nussinov R. Phys Chem Chem Phys. 2013; 15:8868–8877. [PubMed: 23450150]
45. Lim KH, Kim YK, Chang YT. Biochemistry. 2007; 46:13523–13532. [PubMed: 17973493]
46. Noy D, Solomonov I, Sinkevich O, Arad T, Kjaer K, Sagi I. Journal of the American Chemical Society. 2008; 130:1376–1383. [PubMed: 18179213]
47. Zirah S, Kozin SA, Mazur AK, Blond A, Cheminant M, Segalas-Milazzo I, Debey P, Rebuffat S. J Biol Chem. 2006; 281:2151–2161. [PubMed: 16301322]
48. Talmard C, Guilloreau L, Coppel Y, Mazarguil H, Faller P. Chembiochem: a European journal of chemical biology. 2007; 8:163–165. [PubMed: 17195250]
49. Gaggelli E, Janicka-Klos A, Jankowska E, Kozlowski H, Migliorini C, Molteni E, Valensin D, Valensin G, Wieczerzak E. J Phys Chem B. 2008; 112:100–109. [PubMed: 18072760]
50. Parthasarathy S, Long F, Miller Y, Xiao Y, McElheny D, Thurber K, Ma B, Nussinov R, Ishii Y. Journal of the American Chemical Society. 2011; 133:3390–3400. [PubMed: 21341665]
51. Miller Y, Ma B, Nussinov R. Proc Natl Acad Sci U S A. 2010; 107:9490–9495. [PubMed: 20448202]
52. Miller Y, Ma BY, Nussinov R. Coordin Chem Rev. 2012; 256:2245–2252.
53. Siddiqua A, Luo Y, Meyer V, Swanson MA, Yu X, Wei G, Zheng J, Eaton GR, Ma B, Nussinov R, Eaton SS, Margittai M. Journal of the American Chemical Society. 2012; 134:10271–10278. [PubMed: 22656332]
54. Luo Y, Dinkel P, Yu X, Margittai M, Zheng J, Nussinov R, Wei G, Ma B. Chem Commun (Camb). 2013; 49:3582–3584. [PubMed: 23527380]
55. Rosenman DJ, Connors CR, Chen W, Wang C, Garcia AE. Journal of molecular biology. 2013; 425:3338–3359. [PubMed: 23811057]
56. Ball KA, Phillips AH, Wemmer DE, Head-Gordon T. Biophys J. 2013; 104:2714–2724. [PubMed: 23790380]
57. Lin YS, Bowman GR, Beauchamp KA, Pande VS. Biophys J. 2012; 102:315–324. [PubMed: 22339868]
58. Lv Z, Roychaudhuri R, Condron MM, Teplow DB, Lyubchenko YL. Sci Rep. 2013; 3:2880. [PubMed: 24096987]

59. Barz B, Urbanc B. PLoS One. 2012; 7:e34345. [PubMed: 22509291]
60. Cote S, Laghaei R, Derreumaux P, Mousseau N. J Phys Chem B. 2012; 116:4043–4055. [PubMed: 22409719]
61. Zhang T, Zhang J, Derreumaux P, Mu Y. J Phys Chem B. 2013; 117:3993–4002. [PubMed: 23537203]
62. Meral D, Urbanc B. Journal of molecular biology. 2013; 425:2260–2275. [PubMed: 23500806]
63. Miller Y, Ma B, Nussinov R. Chem Rev. 2010; 110:4820–4838. [PubMed: 20402519]
64. Ndlovu H, Ashcroft AE, Radford SE, Harris SA. Biophys J. 2012; 102:587–596. [PubMed: 22325282]
65. Miller Y, Ma B, Tsai CJ, Nussinov R. Proc Natl Acad Sci U S A. 2010; 107:14128–14133. [PubMed: 20660780]
66. Miller Y, Ma B, Nussinov R. Journal of the American Chemical Society. 2011; 133:2742–2748. [PubMed: 21299220]
67. Petkova AT, Yau WM, Tycko R. Biochemistry. 2006; 45:498–512. [PubMed: 16401079]
68. Paravastu AK, Leapman RD, Yau WM, Tycko R. Proc Natl Acad Sci U S A. 2008; 105:18349–18354. [PubMed: 19015532]
69. Meinhardt J, Sachse C, Hortschansky P, Grigorieff N, Fandrich M. Journal of molecular biology. 2009; 386:869–877. [PubMed: 19038266]
70. Zhang R, Hu X, Khant H, Ludtke SJ, Chiu W, Schmid MF, Frieden C, Lee JM. Proc Natl Acad Sci U S A. 2009; 106:4653–4658. [PubMed: 19264960]
71. Rhee SK, Quist AP, Lal R. J Biol Chem. 1998; 273:13379–13382. [PubMed: 9593665]
72. Bhatia R, Lin H, Lal R. FASEB J. 2000; 14:1233–1243. [PubMed: 10834945]
73. Lin H, Bhatia R, Lal R. FASEB J. 2001; 15:2433–2444. [PubMed: 11689468]
74. Lal R, Lin H, Quist AP. Biochim Biophys Acta-Biomembr. 2007; 1768:1966–1975.
75. Mustata M, Capone R, Jang H, Arce FT, Ramachandran S, Lal R, Nussinov R. J Am Chem Soc. 2009; 131:14938–14945. [PubMed: 19824733]
76. Arce FT, Jang H, Ramachandran S, Landon PB, Nussinov R, Lal R. Soft Matter. 2011; 7:5267–5273. [PubMed: 21918653]
77. Connelly L, Arce FT, Jang H, Capone R, Kotler SA, Ramachandran S, Kagan BL, Nussinov R, Lal R. J Phys Chem B. 2012; 116:1728–1735. [PubMed: 22217000]
78. Connelly L, Jang H, Arce FT, Ramachandran S, Kagan BL, Nussinov R, Lal R. Biochemistry. 2012; 51:3031–3038. [PubMed: 22413858]
79. Lashuel HA, Hartley D, Petre BM, Walz T, Lansbury PT Jr. Nature. 2002; 418:291. [PubMed: 12124613]
80. Lashuel HA, Hartley DM, Petre BM, Wall JS, Simon MN, Walz T, Lansbury PT Jr. J Mol Biol. 2003; 332:795–808. [PubMed: 12972252]
81. Lashuel HA, Lansbury PT Jr. Q Rev Biophys. 2006; 39:167–201. [PubMed: 16978447]
82. Qi R, Luo Y, Ma B, Nussinov R, Wei G. Biomacromolecules. 2014; 15:122–131. [PubMed: 24313776]
83. Olubiyi OO, Frenzel D, Bartnik D, Gluck JM, Brener O, Nagel-Steger L, Funke SA, Willbold D, Strodel B. Curr Med Chem. 2013
84. Poojari C, Xiao D, Batista VS, Strodel B. Biophys J. 2013; 105:2323–2332. [PubMed: 24268144]
85. Smith MD, Cruz L. J Phys Chem B. 2013; 117:14907–14915. [PubMed: 24261958]
86. Miller C, Zerze GH, Mittal J. J Phys Chem B. 2013; 117:16066–16075. [PubMed: 24245879]
87. Buchanan LE, Dunkelberger EB, Tran HQ, Cheng PN, Chiu CC, Cao P, Raleigh DP, de Pablo JJ, Nowick JS, Zanni MT. Proc Natl Acad Sci U S A. 2013; 110:19285–19290. [PubMed: 24218609]
88. Guo J, Zhang Y, Ning L, Jiao P, Liu H, Yao X. Biochim Biophys Acta. 2013; 1840:357–366. [PubMed: 24041993]
89. Friedman R, Caflisch A. Proteins. 2014; 82:399–404. [PubMed: 24038616]
90. Xu L, Wang X, Shan S. J Comput Chem. 2013; 34:2524–2536. [PubMed: 24037720]
91. Chiu CC, Singh S, de Pablo JJ. Biophys J. 2013; 105:1227–1235. [PubMed: 24010666]

92. Wu C, Shea JE. PLoS Comput Biol. 2013; 9:e1003211. [PubMed: 24009497]
93. Ndlovu H, Ashcroft AE, Radford SE, Harris SA. Beilstein J Nanotechnol. 2013; 4:429–440. [PubMed: 23946911]
94. Maiorana A, Marino T, Minicozzi V, Morante S, Russo N. Biophys Chem. 2013; 182:86–93. [PubMed: 23932412]
95. Di Scala C, Troadec JD, Lelievre C, Garmy N, Fantini J, Chahinian H. J Neurochem. 2014; 128:186–195. [PubMed: 23919567]
96. Hernandez-Rodriguez M, Correa-Basurto J, Benitez-Cardoza CG, Resendiz-Albor AA, Rosales-Hernandez MC. Protein Sci. 2013; 22:1320–1335. [PubMed: 23904252]
97. Skeby KK, Sorensen J, Schiott B. Journal of the American Chemical Society. 2013; 135:15114–15128. [PubMed: 23859103]
98. Lemkul JA, Bevan DR. Biochemistry. 2013; 52:4971–4980. [PubMed: 23855340]
99. Shea JE, Urbanc B. Curr Top Med Chem. 2012; 12:2596–2610. [PubMed: 23339310]
100. Gessel MM, Wu C, Li H, Bitan G, Shea JE, Bowers MT. Biochemistry. 2012; 51:108–117. [PubMed: 22129303]
101. Yu X, Wang Q, Pan Q, Zhou F, Zheng J. Phys Chem Chem Phys. 2013; 15:8878–8889. [PubMed: 23493873]
102. Liang G, Zhao J, Yu X, Zheng J. Biochemistry. 2013; 52:1089–1100. [PubMed: 23331123]
103. Capone R, Jang H, Kotler SA, Connelly L, Arce FT, Ramachandran S, Kagan BL, Nussinov R, Lal R. J Chem Theory Comput. 2012; 8:1143–1152. [PubMed: 22423218]
104. Capone R, Jang H, Kotler SA, Kagan BL, Nussinov R, Lal R. Biochemistry. 2012; 51:776–785. [PubMed: 22242635]
105. Tofoleanu F, Buchete NV. Prion. 2012; 6:339–345. [PubMed: 22874669]
106. Jang H, Teran Arce F, Ramachandran S, Kagan BL, Lal R, Nussinov R. J Phys Chem B. 2013; 117:11518–11529. [PubMed: 24000923]
107. Zhao J, Luo Y, Jang H, Yu X, Wei G, Nussinov R, Zheng J. Biochim Biophys Acta. 2012; 1818:3121–3130. [PubMed: 22935354]
108. Jang H, Ma B, Lal R, Nussinov R. Biophys J. 2008; 95:4631–4642. [PubMed: 18708452]
109. Capone R, Mustata M, Jang H, Arce FT, Nussinov R, Lal R. Biophys J. 2010; 98:2644–2652. [PubMed: 20513409]
110. Gupta K, Jang H, Harlen K, Puri A, Nussinov R, Schneider JP, Blumenthal R. Biophys J. 2013; 105:2093–2103. [PubMed: 24209854]
111. Brooks BR, Bruccoleri RE, Olafson BD, States DJ, Swaminathan S, Karplus M. J Comp Chem. 1983; 4:187–217.
112. Phillips JC, Braun R, Wang W, Gumbart J, Tajkhorshid E, Villa E, Chipot C, Skeel RD, Kale L, Schulten K. J Comp Chem. 2005; 26:1781–1802. [PubMed: 16222654]
113. Shao H, Jao S, Ma K, Zagorski MG. Journal of molecular biology. 1999; 285:755–773. [PubMed: 9878442]
114. Hou LM, Shao HY, Zhang YB, Li H, Menon NK, Neuhaus EB, Brewer JM, Byeon IJL, Ray DG, Vitek MP, Iwashita T, Makula RA, Przybyla AB, Zagorski MG. Journal of the American Chemical Society. 2004; 126:1992–2005. [PubMed: 14971932]
115. Verdier Y, Zarandi M, Penke B. J Pept Sci. 2004; 10:229–248. [PubMed: 15160835]
116. Shirwany NA, Payette D, Xie J, Guo Q. Neuropsychiatr Dis Treat. 2007; 3:597–612. [PubMed: 19300589]
117. Buchete NV. Biophys J. 2012; 103:1411–1413. [PubMed: 23062332]
118. Walsh DM, Klyubin I, Fadeeva JV, Cullen WK, Anwyl R, Wolfe MS, Rowan MJ, Selkoe DJ. Nature. 2002; 416:535–539. [PubMed: 11932745]
119. Kagan BL. Prog Mol Biol Transl Sci. 2012; 107:295–325. [PubMed: 22482454]
120. Arispe N, Rojas E, Pollard HB. Proc Natl Acad Sci USA. 1993; 90:567–571. [PubMed: 8380642]
121. Arispe N, Pollard HB, Rojas E. Proc Natl Acad Sci USA. 1993; 90:10573–10577. [PubMed: 7504270]
122. Pollard HB, Rojas E, Arispe N. Ann N Y Acad Sci. 1993; 695:165–168. [PubMed: 8239277]

123. Arispe N, Pollard HB, Rojas E. Calcium Hypothesis of Aging and Dementia. 1994; 747:256–266.
124. Arispe N, Pollard HB, Rojas E. Proc Natl Acad Sci U S A. 1996; 93:1710–1715. [PubMed: 8643694]
125. Hirakura Y, Lin MC, Kagan BL. Journal of Neuroscience Research. 1999; 57:458–466. [PubMed: 10440895]
126. Kagan BL, Azimov R, Azimova R. J Membr Biol. 2004; 202:1–10. [PubMed: 15702375]
127. Kagan BL, Hirakura Y, Azimov R, Azimova R, Lin MC. Peptides. 2002; 23:1311–1315. [PubMed: 12128087]
128. Mirzabekov TA, Lin MC, Kagan BL. J Biol Chem. 1996; 271:1988–1992. [PubMed: 8567648]
129. Brender JR, Heyl DL, Samisetti S, Kotler SA, Osborne JM, Pesaru RR, Ramamoorthy A. Phys Chem Chem Phys. 2013; 15:8908–8915. [PubMed: 23493863]
130. Sciacca MF, Milardi D, Messina GM, Marletta G, Brender JR, Ramamoorthy A, La Rosa C. Biophys J. 2013; 104:173–184. [PubMed: 23332070]
131. Sciacca MF, Brender JR, Lee DK, Ramamoorthy A. Biochemistry. 2012; 51:7676–7684. [PubMed: 22970795]
132. Brender JR, Hartman K, Reid KR, Kennedy RT, Ramamoorthy A. Biochemistry. 2008; 47:12680–12688. [PubMed: 18989933]
133. Brender JR, Durr UH, Heyl D, Budarapu MB, Ramamoorthy A. Biochim Biophys Acta. 2007; 1768:2026–2029. [PubMed: 17662957]
134. Lin MC, Mirzabekov T, Kagan BL. J Biol Chem. 1997; 272:44–47. [PubMed: 8995224]
135. Hirakura Y, Azimov R, Azimova R, Kagan BL. Journal of neuroscience research. 2000; 60:490–494. [PubMed: 10797551]
136. Hirakura Y, Kagan BL. Amyloid-J Protein Fold Disord. 2001; 8:94–100.
137. Hirakura Y, Azimova R, Azimov R, Kagan B. Biophys J. 2001; 80:129a–129a.
138. Hirakura Y, Carreras I, Sipe JD, Kagan BL. Amyloid. 2002; 9:13–23. [PubMed: 12000193]
139. Lacor PN, Buniel MC, Furlow PW, Clemente AS, Velasco PT, Wood M, Viola KL, Klein WL. J Neurosci. 2007; 27:796–807. [PubMed: 17251419]
140. De Felice FG, Velasco PT, Lambert MP, Viola K, Fernandez SJ, Ferreira ST, Klein WL. J Biol Chem. 2007; 282:11590–11601. [PubMed: 17308309]
141. De Felice FG, Wu D, Lambert MP, Fernandez SJ, Velasco PT, Lacor PN, Bigio EH, Jerecic J, Acton PJ, Shughrue PJ, Chen-Dodson E, Kinney GG, Klein WL. Neurobiol Aging. 2008; 29:1334–1347. [PubMed: 17403556]
142. Kayed R, Sokolov Y, Edmonds B, McIntire TM, Milton SC, Hall JE, Glabe CG. J Biol Chem. 2004; 279:46363–46366. [PubMed: 15385542]
143. Sokolov Y, Kozak JA, Kayed R, Chanturiya A, Glabe C, Hall JE. J Gen Physiol. 2006; 128:637–647. [PubMed: 17101816]
144. Schauerte JA, Wong PT, Wisser KC, Ding H, Steel DG, Gafni A. Biochemistry. 2010; 49:3031–3039. [PubMed: 20201586]
145. Sciacca MFM, Kotler SA, Brender JR, Chen J, Lee DK, Ramamoorthy A. Biophys J. 2012; 103:702–710. [PubMed: 22947931]
146. Sciacca MFM, Brender JR, Lee DK, Ramamoorthy A. Biochemistry. 2012; 51:7676–7684. [PubMed: 22970795]
147. Milanesi L, Sheynis T, Xue WF, Orlova EV, Hellewell AL, Jelinek R, Hewitt EW, Radford SE, Saibil HR. Proc Natl Acad Sci USA. 2012; 109:20455–20460. [PubMed: 23184970]
148. Lazo ND, Grant MA, Condron MC, Rigby AC, Teplow DB. Protein Science. 2005; 14:1581–1596. [PubMed: 15930005]
149. Crescenzi O, Tomaselli S, Guerrini R, Salvadori S, D'Ursi AM, Temussi PA, Picone D. Eur J Biochem. 2002; 269:5642–5648. [PubMed: 12423364]
150. Tomaselli S, Esposito V, Vangone P, van Nuland NAJ, Bonvin AMJJ, Guerrini R, Tancredi T, Temussi PA, Picone D. Chembiochem. 2006; 7:257–267. [PubMed: 16444756]
151. Vivekanandan S, Brender JR, Lee SY, Ramamoorthy A. Biochem Biophys Res Commun. 2011; 411:312–316. [PubMed: 21726530]

152. Lührs T, Ritter C, Adrian M, Riek-Loher D, Bohrmann B, Doeli H, Schubert D, Riek R. Proc Natl Acad Sci USA. 2005; 102:17342–17347. [PubMed: 16293696]
153. Ma B, Nussinov R. Proc Natl Acad Sci U S A. 2002; 99:14126–14131. [PubMed: 12391326]
154. Bertini I, Gonnelli L, Luchinat C, Mao J, Nesi A. Journal of the American Chemical Society. 2011; 133:16013–16022. [PubMed: 21882806]
155. Lu JX, Qiang W, Yau WM, Schwieters CD, Meredith SC, Tycko R. Cell. 2013; 154:1257–1268. [PubMed: 24034249]
156. Chimon S, Shaibat MA, Jones CR, Calero DC, Aizezi B, Ishii Y. Nat Struct Mol Biol. 2007; 14:1157–1164. [PubMed: 18059284]
157. Wu JW, Breydo L, Isas JM, Lee J, Kuznetsov YG, Langen R, Glabe C. J Biol Chem. 2010; 285:6071–6079. [PubMed: 20018889]
158. Ladiwala AR, Litt J, Kane RS, Aucoin DS, Smith SO, Ranjan S, Davis J, Vannostrand WE, Tessier PM. J Biol Chem. 2012; 287:24765–24773. [PubMed: 22547072]
159. Jang H, Connelly L, Arce FT, Ramachandran S, Kagan BL, Lal R, Nussinov R. J Chem Theory Comput. 2013; 9:822–833. [PubMed: 23316126]
160. Ciccotosto GD, Tew DJ, Drew SC, Smith DG, Johanssen T, Lal V, Lau TL, Perez K, Curtain CC, Wade JD, Separovic F, Masters CL, Smith JP, Barnham KJ, Cappai R. Neurobiol Aging. 2011; 32:235–248. [PubMed: 19324459]
161. de Groot NS, Aviles FX, Vendrell J, Ventura S. FEBS J. 2006; 273:658–668. [PubMed: 16420488]
162. Wang Z, Natte R, Berliner JA, van Duinen SG, Vinters HV. Stroke. 2000; 31:534–538. [PubMed: 10657433]
163. Nilsberth C, Westlind-Danielsson A, Eckman CB, Condron MM, Axelman K, Forsell C, Stenh C, Luthman J, Teplow DB, Younkin SG, Naslund J, Lannfelt L. Nat Neurosci. 2001; 4:887–893. [PubMed: 11528419]
164. Miravalle L, Tokuda T, Chiarle R, Giaccone G, Bugiani O, Tagliavini F, Frangione B, Ghiso J. J Biol Chem. 2000; 275:27110–27116. [PubMed: 10821838]
165. Levy E, Carman MD, Fernandez-Madrid IJ, Power MD, Lieberburg I, van Duinen SG, Bots GT, Luyendijk W, Frangione B. Science. 1990; 248:1124–1126. [PubMed: 2111584]
166. Grabowski TJ, Cho HS, Vonsattel JP, Rebeck GW, Greenberg SM. Ann Neurol. 2001; 49:697–705. [PubMed: 11409420]
167. Viet MH, Li MS. J Chem Phys. 2012; 136:245105. [PubMed: 22755606]
168. Wise-Scira O, Xu L, Kitahara T, Perry G, Coskuner O. J Chem Phys. 2011; 135:205101. [PubMed: 22128957]
169. Thirumalai D, Reddy G, Straub JE. Acc Chem Res. 2012; 45:83–92. [PubMed: 21761818]
170. Paparcone R, Pires MA, Buehler MJ. Biochemistry. 2010; 49:8967–8977. [PubMed: 20731379]
171. Davis CH, Berkowitz ML. J Phys Chem B. 2009; 113:14480–14486. [PubMed: 19807060]
172. Reddy G, Straub JE, Thirumalai D. J Phys Chem B. 2009; 113:1162–1172. [PubMed: 19125574]
173. Krone MG, Baumketner A, Bernstein SL, Wyttenbach T, Lazo ND, Teplow DB, Bowers MT, Shea JE. Journal of molecular biology. 2008; 381:221–228. [PubMed: 18597778]
174. Fawzi NL, Phillips AH, Ruscio JZ, Doucleff M, Wemmer DE, Head-Gordon T. Journal of the American Chemical Society. 2008; 130:6145–6158. [PubMed: 18412346]
175. Walsh DM, Lomakin A, Benedek GB, Condron MM, Teplow DB. J Biol Chem. 1997; 272:22364–22372. [PubMed: 9268388]
176. Williams AD, Portelius E, Kheterpal I, Guo JT, Cook KD, Xu Y, Wetzel R. Journal of molecular biology. 2004; 335:833–842. [PubMed: 14687578]
177. Tomiyama T, Nagata T, Shimada H, Teraoka R, Fukushima A, Kanemitsu H, Takuma H, Kuwano R, Imagawa M, Ataka S, Wada Y, Yoshioka E, Nishizaki T, Watanabe Y, Mori H. Ann Neurol. 2008; 63:377–387. [PubMed: 18300294]
178. Murakami K, Irie K, Morimoto A, Ohigashi H, Shindo M, Nagao M, Shimizu T, Shirasawa T. J Biol Chem. 2003; 278:46179–46187. [PubMed: 12944403]
179. Jawhar S, Wirths O, Bayer TA. J Biol Chem. 2011; 286:38825–38832. [PubMed: 21965666]

180. Saido TC, Iwatsubo T, Mann DM, Shimada H, Ihara Y, Kawashima S. Neuron. 1995; 14:457–466. [PubMed: 7857653]

181. Poojari C, Kukol A, Strodel B. Biochimica et Biophysica Acta (BBA) - Biomembranes. 2012; 1828:327–339. [PubMed: 22975281]

182. DeMuro A, Smith M, Parker I. J Cell Biol. 2011; 195:515–524. [PubMed: 22024165]

183. Kagan BL, Thundimadathil J. Adv Exp Med Biol. 2010; 677:150–167. [PubMed: 20687488]

184. Smart OS, Goodfellow JM, Wallace BA. Biophys J. 1993; 65:2455–2460. [PubMed: 7508762]

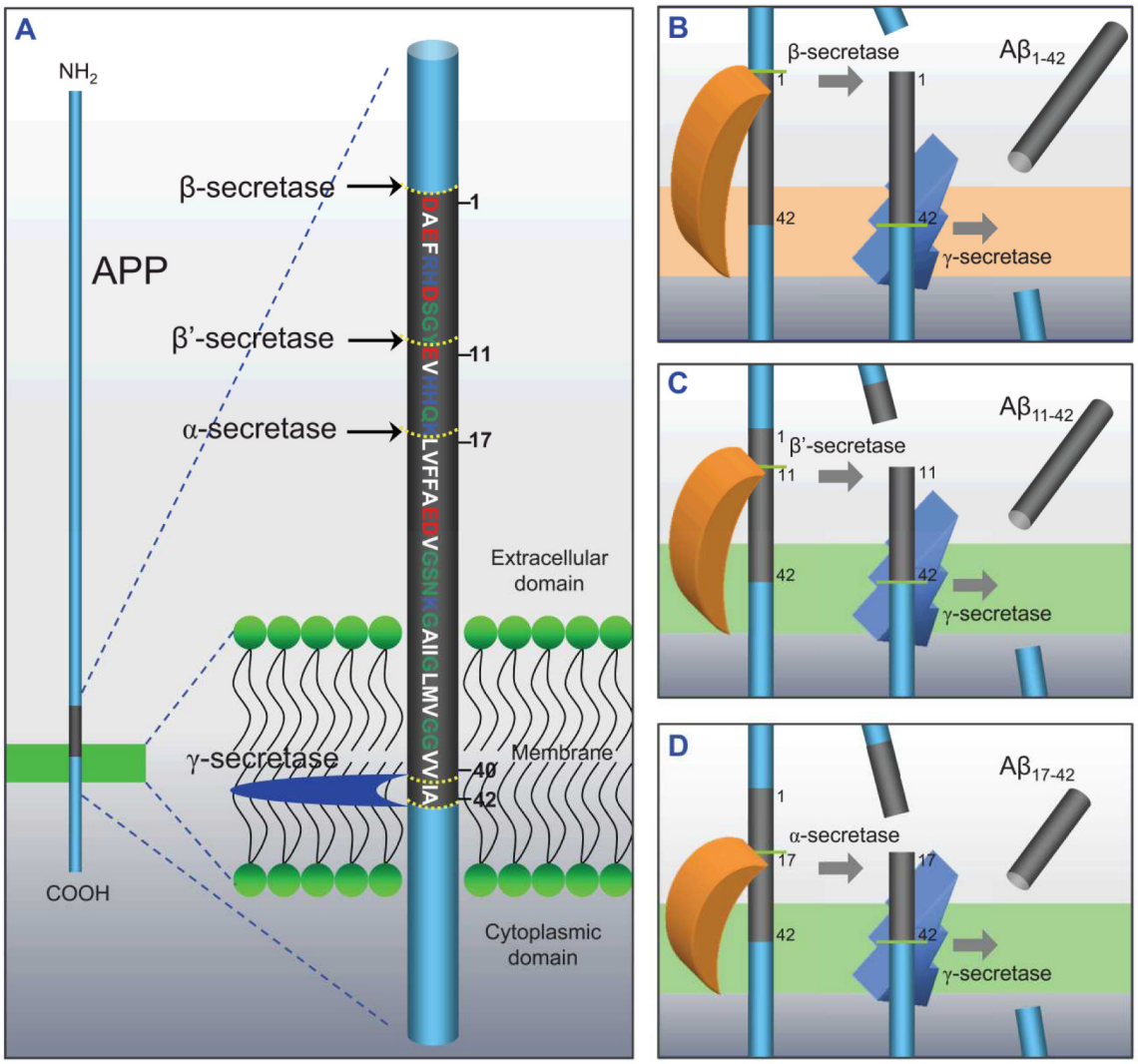

Figure 1.

Productions of β-amyloid (Aβ) via various cleavages. (A) A cartoon representing the cleavage process by α-, β-, β′- and γ-secretases of amyloid precursor protein (APP). The $Aβ_{1-42}$ domain is shown in gray with the sequence and numbering of the amino acids. In single letter amino acid codes, hydrophobic, polar/Gly, positively charged, and negatively charged residues are colored white, green, blue, and red, respectively. Various Aβ fragments are processed by different secretase combinations. (B) Amyloidogenic fragment of $Aβ_{1-40/42}$ by β- and γ-secretases, and non-amyloidogenic fragments of (C) $Aβ_{11-40/42}$ by β′- and γ-secretases and (D) $Aβ_{17-40/42}$ by α- and γ-secretases. These cartoons were inspired by previous publication.[31] (B and D from Jang *et al*., 2010,[37] are reprinted with permission).

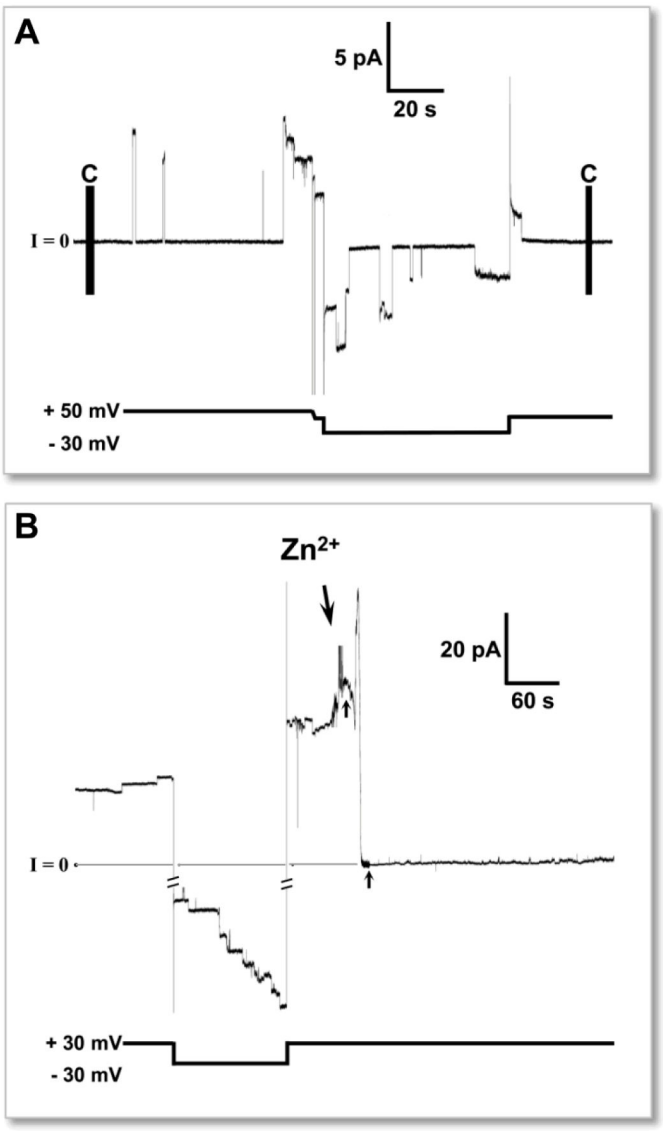

Figure 2.

An example of stepwise current feature across planar lipid bilayer (PLB, or BLM representing “black lipid membrane”) membrane produced by amyloid channels. (A) The electrophysiological activity of $A\beta_{1\text{-}42}$ ion channels embedded in PLB. (B) Inhibition of channel activity by Zn^{2+} addition. Time of Zn^{2+} addition (2 mM) is marked by arrow. (From Capone *et al*., 2012,[103] reprinted with permission).

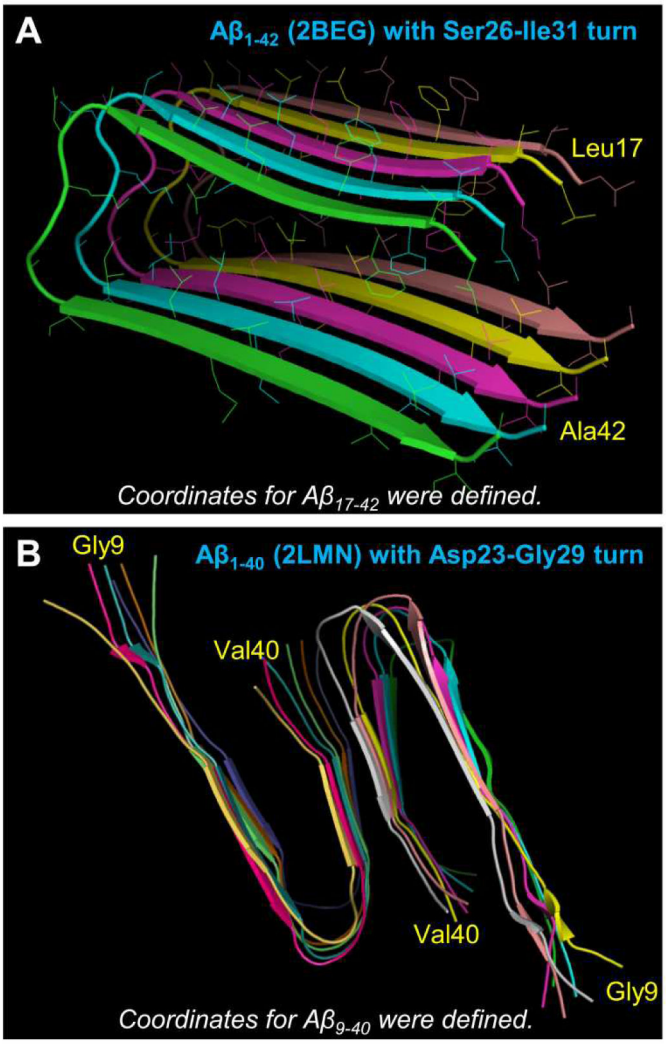

Figure 3.

Three-dimensional structures of Alzheimer's amyloids. (A) The pentameric $A\beta_{1\text{-}42}$ fibril structure obtained from a combination of hydrogen/deuterium-exchange nuclear magnetic resonance (NMR) data, side-chain packing constraints from pairwise mutagenesis, solid state NMR (ssNMR) and electron microscopy (EM) (pdb id: 2BEG).[152] The coordinates for residues 1–16 were missing due to disorder. (B) The ssNMR model for small $A\beta_{1\text{-}40}$ protofibrils (pdb ids: 2LMN).[67] The coordinates for residues 1–8 were missing due to disorder. Residues at both termini are marked.

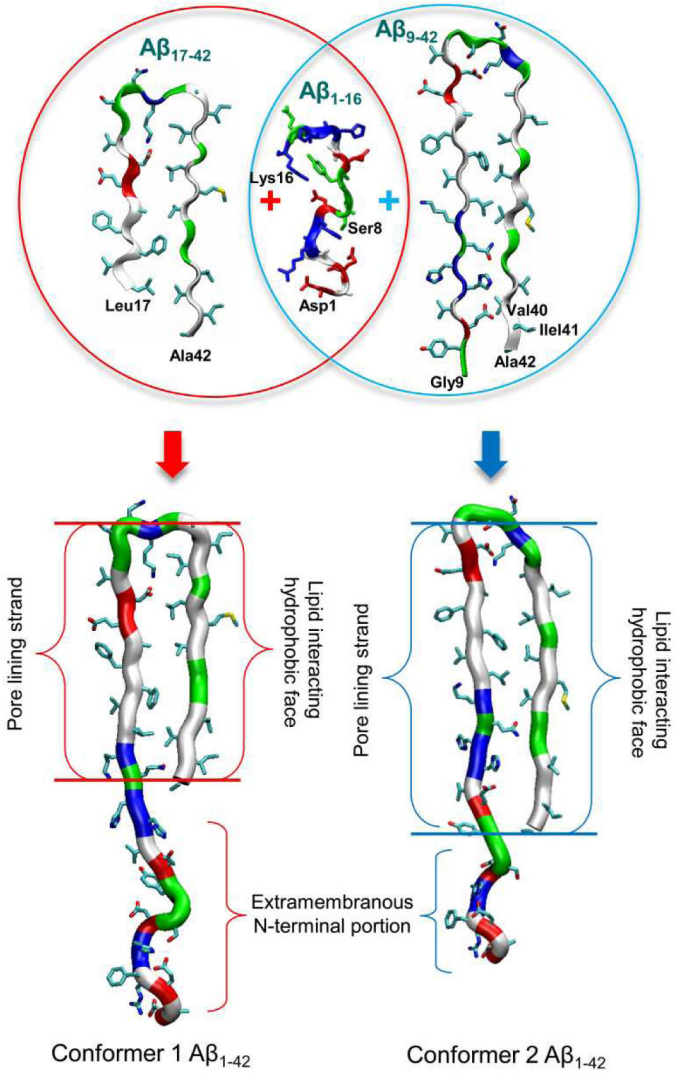

Figure 4.

A cartoon representing the constructions of the full-length $A\beta_{1-42}$ peptides. The N-terminal truncated Aβ monomers are U-shape with the β-strand-turn-β-strand motif. The missing N-terminal portions of these NMR-derived Aβ peptides are recovered with the coordinates from the solution structure of $A\beta_{1-16}$ (pdb id: 1ZE7).[47] By covalently connecting the N-terminal to the truncated Aβ peptides, two $A\beta_{1-42}$ conformers (conformer 1 and 2) with different turns can be generated.

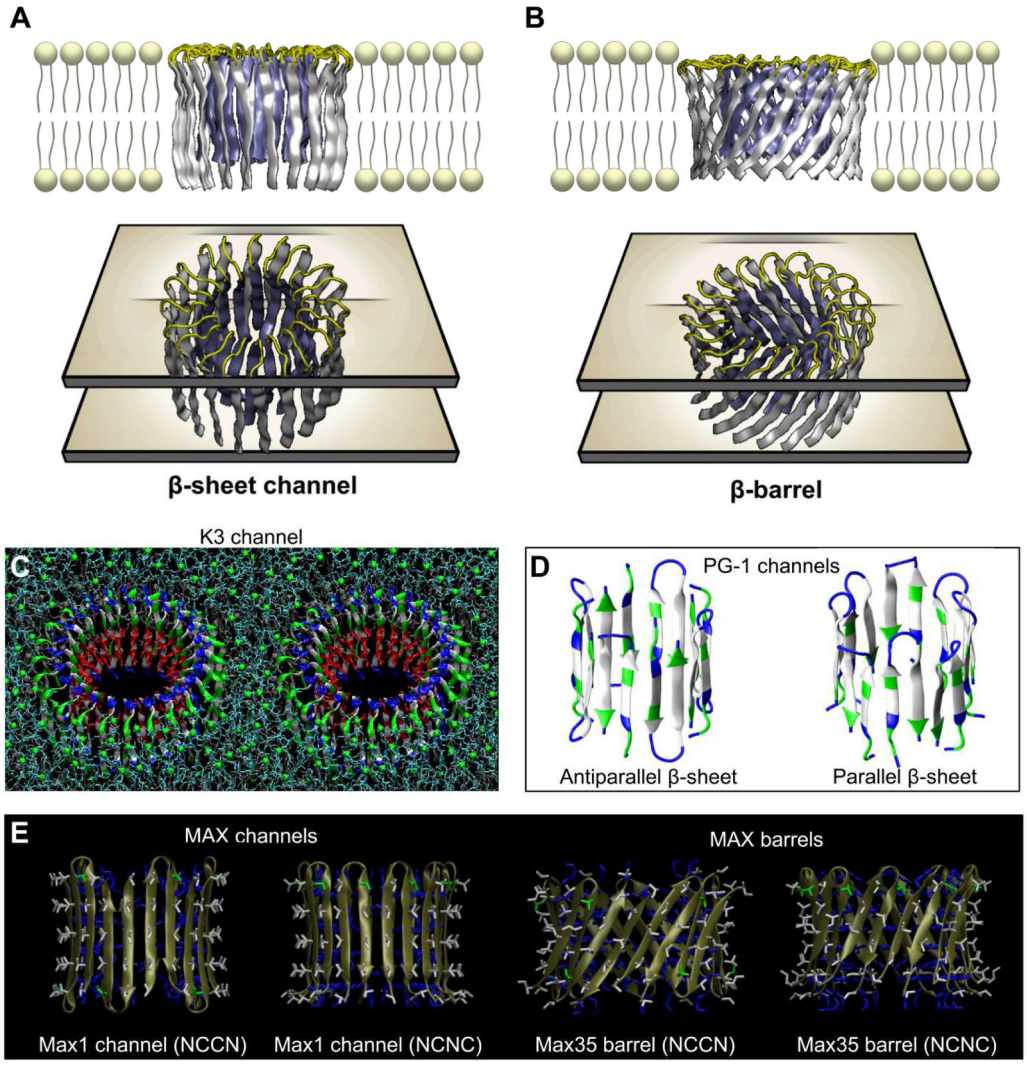

Figure 5.

Conventional β-sheet channel vs. β-barrel designs. (A) The conventional β-sheet channel has the β-strands that orient parallel to the membrane normal, (B) while the β-strands that orient obliquely to the membrane normal generate β-barrel structure. Above examples are shown for the p3 ($A\beta_{17-42}$) channel and barrel. Other examples of the β-sheet channel and barrel formed by the U-shaped K3 (a fragment of β_2-microglobulin) peptide and by the PG-1 and MAX β-hairpins. (C) The 24-mer channel embedded in the DOPC bilayer in stereo view.[75] (D) The 8-mer PG-1 channels with the antiparallel and parallel β-strand arrangements.[108] (E) The 10-mer antiparallel MAX channels and barrels in the NCCN and NCNC packing modes (from Gupta *et al.*, 2013,[110] reprinted with permission).

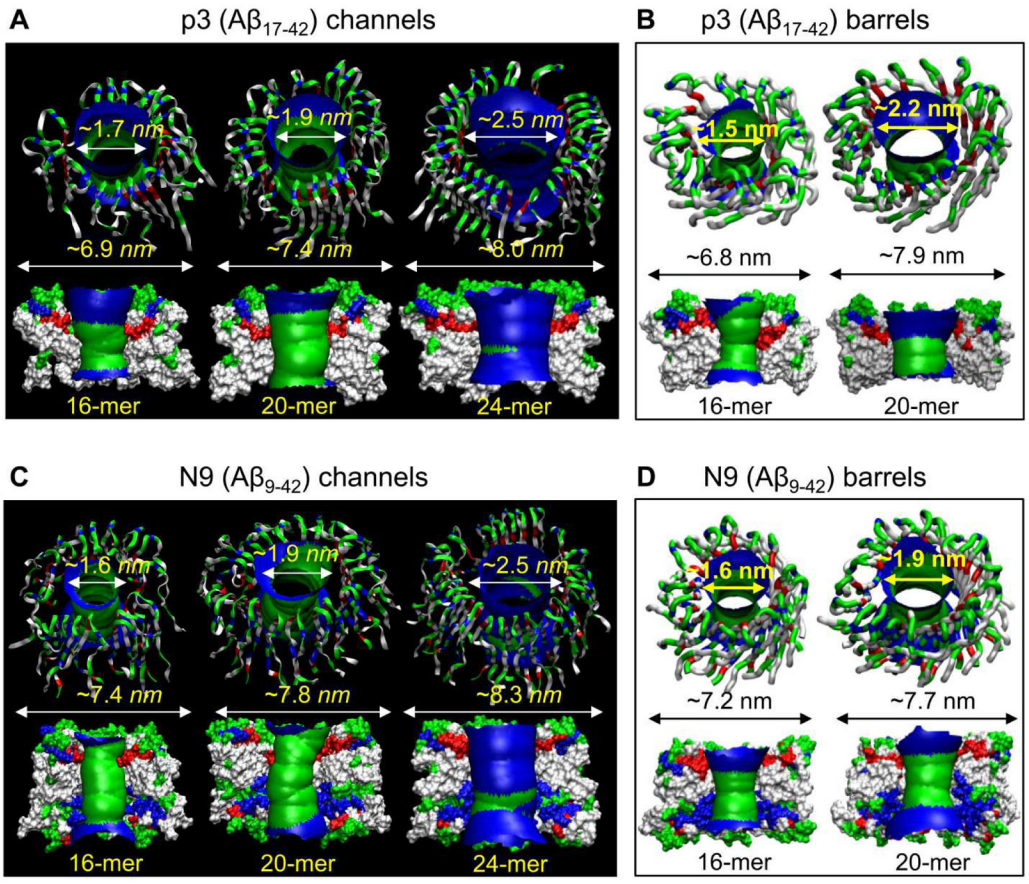

Figure 6.

Truncated Aβ channel/barrel conformations in the lipid bilayer. Averaged pore structures calculated by the HOLE program[184] embedded in the averaged channel/barrel conformations during the simulations for the p3 ($A\beta_{17-42}$) (A) channels and (B) barrels, and the N9 ($A\beta_{9-42}$) (C) channels and (D) barrels. (A from Jang *et al.*, 2010,[37] B and D from Jang *et al.*, 2010,[38] and C from from Jang *et al.*, 2009,[35] reprinted with permission).

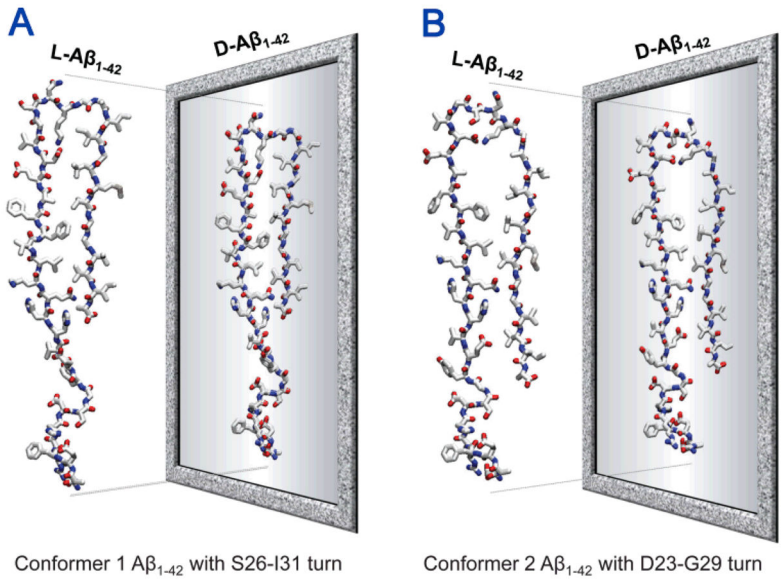

Figure 7.

Schematic diagrams representing the all L- and all-D-amino acids $A\beta_{1-42}$ peptides with different conformers. The coordinates of all D-amino acids $A\beta_{1-42}$ are mirror-imaged coordinates of all L-amino acids $A\beta_{1-42}$ for (A) the conformer 1 and (B) the conformer 2. The standard CHARMM[111] force can be directly used for D-amino acids. However, the parameters include the dihedral angle cross-term map (CMAP), which, for D-amino acids, needs to be corrected since the map was constructed for L-amino acids. To simulate D-amino acids, corrected CMAP data for D-amino acids should be applied via reflecting the phi-psi CMAP matrix for L-amino acids.[77,103,110]

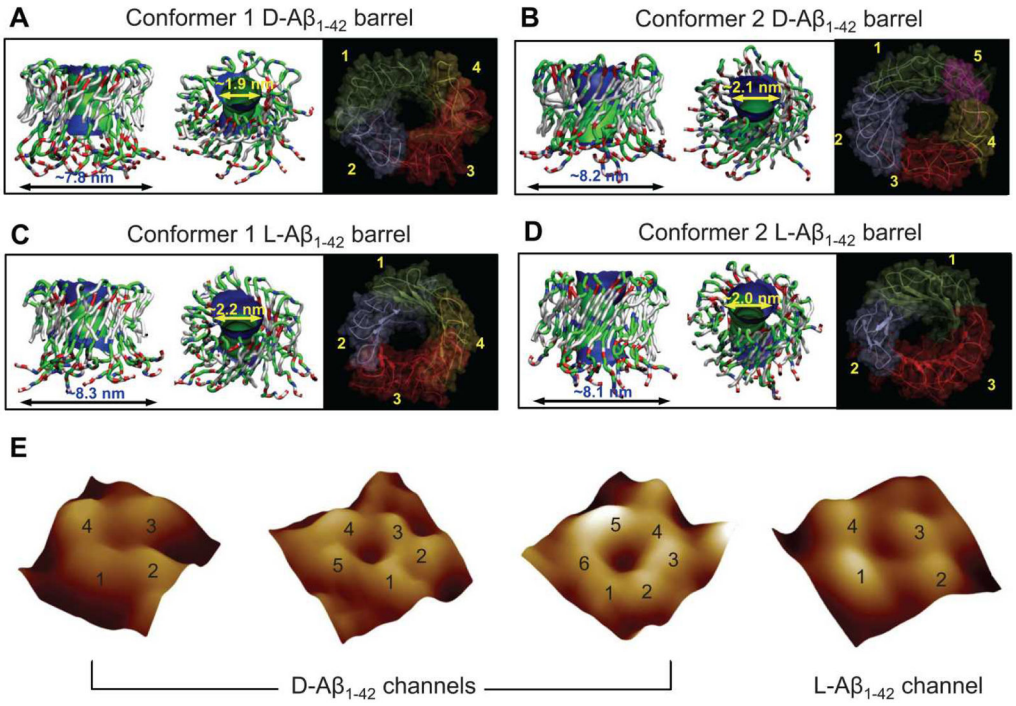

Figure 8.

Full-length $A\beta_{1-42}$ barrel conformations in the lipid bilayer. Simulated barrel structure with an embedded pore structure and highlighted subunits for (A) the conformer 1 and (B) the conformer 2 D-$A\beta_{1-42}$ barrels, and (C) the conformer 1 and (D) the conformer 2 L-$A\beta_{1-42}$ barrels. (E) High resolution atomic force microscopy (AFM) images of D- and L-$A\beta_{1-42}$ reconstituted in the lipid bilayer. The number of subunits is resolved and indicated for each channel. (From Connelly *et al.*, 2012,[77] reprinted with permission).

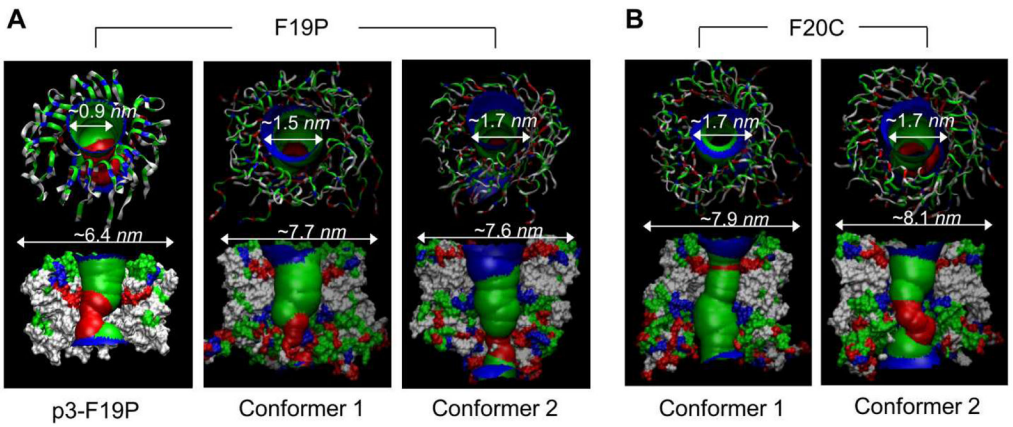

Figure 9.

Aβ mutant channels/barrels in the lipid bilayers. (A) Simulated channel/barrel structures with an embedded pore structure for the p3-F19P (from the truncated $A\beta_{17-42}$) mutant channel (left panel, from Jang *et al.*, 2010,[36] reprinted with permission) and for the conformer 1 and the conformer 2 F19P (from the full-length $A\beta_{1-42}$) mutant barrels (middle and right panels, from Connelly *et al.*, 2012,[78] reprinted with permission). (B) Simulated barrel structures with an embedded pore structure for the conformer 1 and the conformer 2 F20C (from the full-length $A\beta_{1-42}$) mutant barrels (from Connelly *et al.*, 2012,[78] reprinted with permission).

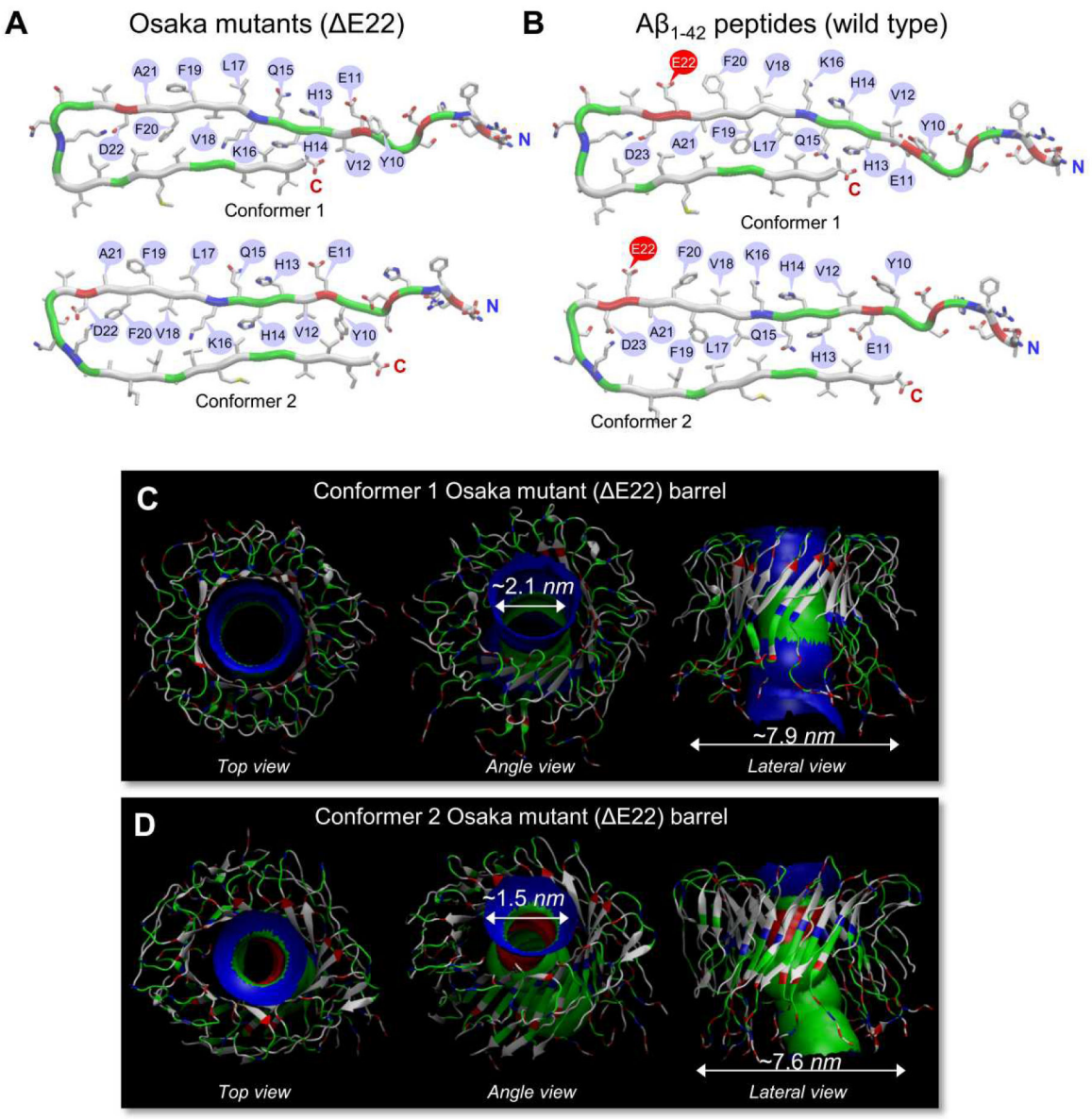

Figure 10.

Osaka mutant (ΔE22) barrels in the lipid bilayers. (A) Monomer conformations of the Osaka mutant with different turns at Ser25-Ile30 (conformer 1) and Asp22-Gly28 (conformer 2). (B) The U-shaped monomer conformations are similar to the wild type $A\beta_{1-42}$ peptides with different turns at Ser26-Ile31 (conformer 1) and Asp23-Gly29 (conformer 2). Simulated barrel structures with an embedded pore structure for (C) the conformer 1 and (D) the conformer 2 Osaka mutant (ΔE22) barrels. (From Jang *et al.*, 2013,[106] reprinted with permission).

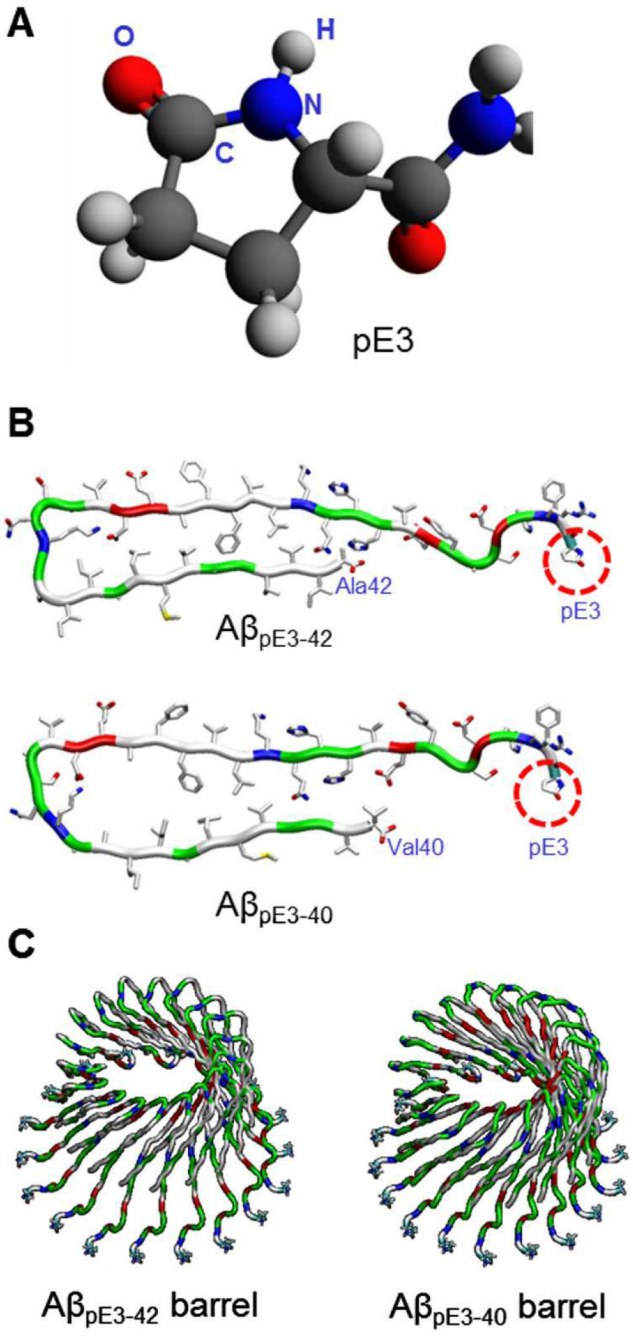

Figure 11.

Computational modelling of pyroglutamate (pE) modified Aβ barrels. (A) Molecular structure of pyroglutamate (pE) at position 3. (B) Monomer conformations of $A\beta_{pE3\text{-}42}$ (upper) and $A\beta_{pE3\text{-}40}$ (lower) peptides. (C) Modelled structures of 18-mer $A\beta_{pE3\text{-}42}$ (left) and $A\beta_{pE3\text{-}40}$ (right) barrels.

Table 1

Structural features of the p3 ($A\beta_{17-42}$) channels/barrels embedded in various lipid bilayers.

p3 ($A\beta_{17-42}$)	Outer diameter (nm)	Pore diameter (nm)	Pore status	Number of subunits	Embedded lipid	Reference
12-mer channel	~6.1	~0.8	collapsed	-	DOPC	37
16-mer channel	~6.8–6.9	~1.7	opened	4, 5	DOPC	36,37
20-mer channel	~7.4	~1.9	opened	5	DOPC	37
24-mer channel	~8.0	~2.5–2.7	opened	3,5	DOPC POPC/POPG=4:1	33,34,37
36-mer channel	~9.3	~3.9	reduced	6	DOPC	37
12-mer barrel	~6.7	~1.8	opened	3	DOPC	38
16-mer barrel	~6.8	~1.5	opened	5	DOPC	38
20-mer barrel	~7.3–7.9	~1.7–2.2	opened	4,5	DOPC	38

Table 2

Structural features of the N9 ($A\beta_{9-42}$) channels/barrels embedded in various lipid bilayers.

N9 ($A\beta_{9-42}$)	Outer diameter (nm)	Pore diameter (nm)	Pore status	Number of subunits	Embedded lipid	Reference
12-mer channel	~6.6	~0.6	collapsed	2	DOPC	35
16-mer channel	~7.3–7.4	~1.5–1.7	opened	5	DOPC	35,36
20-mer channel	~7.8	~1.9	opened	3	DOPC	35
24-mer channel	~7.8–8.3	~2.2–2.5	opened	4,5	DOPC POPC/POPG=4:1	34,35
36-mer channel	~10.3	~3.7	reduced	6	DOPC	35
12-mer barrel	~6.6	~1.3	opened	3	DOPC	38
16-mer barrel	~7.2	~1.6	opened	4	DOPC	38
20-mer barrel	~7.7–8.0	~1.9	opened	5,6	DOPC	38

Table 3

Structural features of the 18-mer $A\beta_{1-42}$ barrels composed of both Aβ conformer 1 and 2 and/or both L- and D-Aβ isomers in various lipid bilayers.

18-mer $A\beta_{1-42}$ barrel	Outer diameter (nm)	Pore diameter (nm)	Pore status	Number of subunits	Embedded lipid	Reference
Conformer 1 (L-isomer)	~7.9–8.3	~1.8–2.2	opened	4	DOPC DOPS/POPE=1:2	77,78,106
Conformer 1 (D-isomer)	~7.8	~1.9	opened	4	DOPS/POPE=1:2	77
Conformer 2 (L-isomer)	~8.0–8.1	~1.9–2.2	opened	3	DOPC DOPS/POPE=1:2	77,78,106
Conformer 2 (D-isomer)	~8.2	~2.1	opened	5	DOPS/POPE=1:2	77

Table 4

Structural features of the p3 ($A\beta_{17-42}$) F19P mutant channel, the full-length ($A\beta_{1-42}$) F19P and F20C barrels, and the Osaka mutant (ΔE22) barrels with an absence of Glu22 in various lipid bilayers.

Aβ mutant channel/barrel	Outer diameter (nm)	Pore diameter (nm)	Pore status	Number of peptides	Embedded lipid	Reference
p3-F19P channel	~6.4	~0.9	clogged up	16	DOPC	36
F19P barrel (Conformer 1)	~7.7	~1.5	clogged up	18	DOPS/POPE=1:2	78,104
F19P barrel (Conformer 2)	~7.6	~1.7	collapsed	18	DOPS/POPE=1:2	78,104
F20C barrel (Conformer 1)	~7.9	~1.7	opened	18	DOPS/POPE=1:2	78,104
F20C barrel (Conformer 2)	~8.1	~1.7	partially collapsed	18	DOPS/POPE=1:2	78,104
ΔE22 barrel (Conformer 1)	~7.9	~2.1	opened	18	DOPC	106
ΔE22 barrel (Conformer 2)	~7.6	~1.5	reduced	18	DOPC	106